# Gapped Dirac cone of antiferromagnetic topological insulator MnBi2Te4

Estyunin D.A.
Saint-Petersburg State University
P-2019b July 2019 - December 2019
Prof. Alexander Shikin (SPBU, Saint-Petersburg, Russia)
Dr. Andrey Varykhalov (Helmholtz Zentrum Berlin, Germany)

## Introduction

To this date a lot of achievements have been done in the field of topologically non-trivial materials. One of them is the theoretical classification and experimental realization of topological insulators (TI). These bulk insulating materials, host metallic surface states, so called topological surface states (TSS), which are characterized by Dirac cone electronic structure. They host electrons with their momentum locked to their spin [1]. This spin-momentum locking forbids back scattering for TSS electrons until time reversal symmetry (TRS) is preserved. However, when TRS is broken in a TI the rise of novel properties has been predicted. The most remarkable is the realization the quantum Hall effect without applied external magnetic field, so called quantum anomalous Hall effect (QAHE) [2, 3].

When TRS is broken by exchange interaction (in case of induced magnetism) the TSS are no longer protected and the Dirac point (DP) gap opens [4]. There are following ways to induce magnetism into TIs: doping with magnetic atoms [5], the proximity effect [6], magnetic extension of TI crystal structure [7] or creation of intrinsic magnetic TI [8]. To this date, the only one with experimentally observed QAHE [3] was doping of 3D TI $(Bi,Sb)_2(Te,Se)_3$ with various magnetic elements (Mn,V,Co,Cr,Gd etc.). However, the highest observed critical temperature required for QAHE is limited by 1 K [9] which may be caused by arbitrary localization of magnetic atoms. Temperature of the TI transition to the QAHE regime relates to the size of the DP band gap and TI's magnetic ordering temperature.

Several remarkable experimental observations and theoretical predictions recently made exploiting the property of antiferromagnetism indicate clearly that antiferromagnetic (AFM) systems can be of great practical importance [10]. As opposed to FM materials, antiferromagnets are robust against external magnetic perturbations and do not produce stray fields. Moreover, such effects as magnetoresistance, spin torque, and ultrafast dynamics observed in certain AFM systems promise significant advances in spin transfer electronics. At the crossroad of antiferromagnetism and the emerging field of "topotronics", i.e. electronics based on the properties of topologically nontrivial systems, an AFM topological insulator (AFMTI) arises.

The existence of AFMTI with $Z_2$ topological classification was previously predicted [11]. An AFMTI can be realized in materials breaking both time-reversal Θ and primitive-lattice translational symmetry $T_{1/2}$ but preserving their combination $S = \Theta\, T_{1/2}$. It was theoretically and experimentally shown that $MnBi_2Te_4$ (Te-Bi-Te-Mn-Te-Bi-Te) satisfies the conditions to be categorized as an AFMTI [8]. According to number of theoretical predictions and direct magnetic measurements its Neel temperature is about 25 K. Below Tn it is expected that S-symmetry breaking should lead to the opening giant band gap at the Dirac point of ~80 meV. Therefore, the recently discovered intrinsic antiferromagnetic (AFM) TI $MnBi_2Te_4$ (MBT) [8] has a great potential to show a high-temperature QAHE.

In the current work we have carried out a detailed analysis of the topological surface states in AFM stoichiometric TI MnBi2Te4 by Spin and Angle-resolved Photoemission spectroscopy (ARPES). We present ARPES spectra measured at 1 K with linear and circular polarization and photon energy of 30 eV. We study spin structure of the Dirac cone by means spin ARPES with laser (hv = 6 eV) photoexcitation. Additionally we analyze distribution of Mn states in the vicinity of TSS applying resonant PES.

## Results and Discussion

In order to analyze electronic structure of the TSS we measured detailed ARPES dispersions E (kx) along ΓK direction of the Brillion zone – Fig.1a. Γ-point position (along ky) was determined by measuring mappings E(kx,ky). One can see that the dispersion has a shape of the cone with intensity dip between upper and lower parts of the cone. It is also visible from energy distribution curve (EDC) in right part of panel (a) which was cut at the Γ-point (as shown by blue lines dispersion image in (a)). The intensity dip appears at about 0.25 eV binding energy. Spectrum in the Fig.1(a) was measured at 1 K which is significantly lower than AFM transition temperature (T = 25 K). Therefore, we can assume magnetism existence in the system. Nevertheless, the mentioned intensity dip rather corresponds to the bulk band gap than the Dirac point band gap. From the EDC profile one can see that maximums of peaks (shown by black arrows), which are related to the gap edges, stand apart for about 0.17 eV. This value significantly exceeds theoretical prediction for the Dirac point band gap (80 meV) but remains smaller than predicted size for bulk band gap. Therefore, we can assume intermixing of the bulk and the TSS state in the dispersion image due to lack of resolution.

We also make an analysis of the electronic structure under photoexcitation by circular polarized light. Difference of spectrum with negative (c-) and positive (c+) polarization reveals circular dichroism (CD) shown in fig.1(b). Photoexcitation under light with c- and c+ polarization is sensitive to total orbital momentum of electron state. For the TSS in TI CD ARPES measurements can show intensity redistribution as in case spin resolved measurements regarding to in-plane spin component. Thus, in fig.1(b) one can see that the branches of the Dirac cone have opposite total orbital moment and, therefore, can be spin polarized. It worth to mentioned, that analysis of cone branches in-plane spin polarization is a one way to experimentally prove their topological origin.

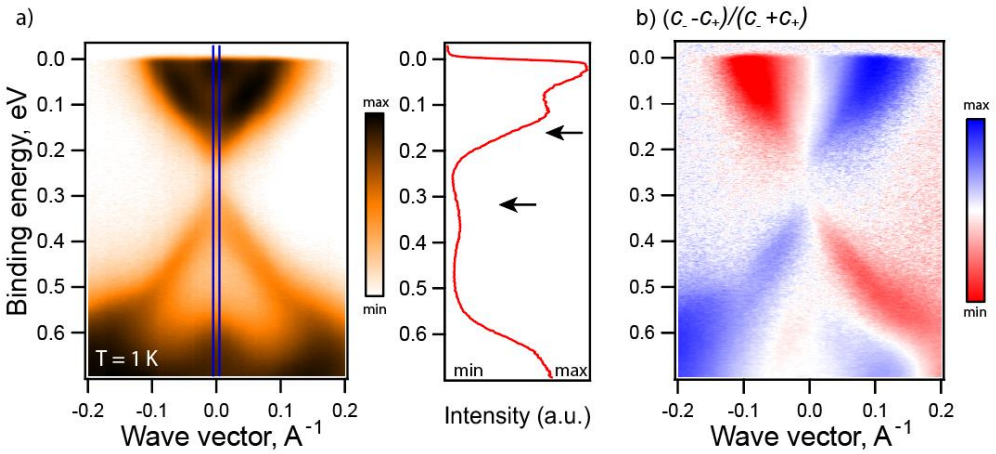


**Fig.1** ARPES dispersion measured at 1-cubed endstation with sample temperature T = 1 K with photoexcitation by synchrotron radiation hv = 30 eV (a). Intensity scale is presented at the right side of the dispersion panel. In the right part of panel (a) EDC at the Γ-point is presented. Corresponding position of the EDC is shown by blue lines in the dispersion image. Black arrows mark the edge of the intensity dip that appears between upper and lower parts of the Dirac cone. (b) circular dichroism obtained as difference between negative (c-) and positive (c+) polarizations with normalization to their sum. Intensity scale is shown at the right part of the panel. Spectra with c+ and c- polarization were measured at T = 1 K and hv = 30 eV.

CD ARPES measurements reveal only plausible image of in-plane spin polarization, since total angular moment is similar with spin in case of absence of the Dirac cone distortion. With intension to probe spin polarization we made spin resolved ARPES with in-plane and out-of-plane direction of spin – Fig.2. Out-of-plane spin direction is perpendicular to sample cleavage surface, in-plane is along surface and perpendicular wave vector, so called Rashba spin component. Since electron spin is locked to its momentum the second in plane component should be zero but it also appears in case of undistorted Dirac cone. Experimentally it realizes in the vicinity of the Dirac point where the TSS has almost the cone shape.

We use laser source of photos with hv = 6 eV and 3D Mott detector at RGBL II endstation of Bessy II synchrotron (see Method section). In Fig.2(a) spin integrated dispersion is presented. Blue and yellow curves mark edges of bottom and top parts of the Dirac cone. We performed spin resolved measurements along K-Γ-K direction of the Brillion zone within $k_{II}$=±0.1 $A^{-1}$. In panels (c) and (d) one can see polarization of out-of-plane and in-plane components for various $k_{II}$. Spin polarizations were plot as $P = \frac{N_{up}-N_{down}}{N_{up}+N_{down}}$. Here $N_{up}$ and $N_{down}$ are intensities from opposite Mott detectors corresponding chosen direction (in-plane or out-of-plane). In panel (d) one can see that the electronic state has invested in-plane spin structure respect to the Γ-point similar with CD ARPES. This proves their topological nature. Out-of-plane spin component shows nonzero signal within the region. It has slight variation in the vicinity of the Fermi level. Presence of inverted out-of-plane component regarding to the Dirac point evidences the “Hedgehog” spin structure and the opening of magnetic Dirac point band gap. Nevertheless, in case of model scenario out-of-plane polarization should inly exist near the Γ-point and decrease while moving away it.

In panel (b) we plot spin up (yellow) and spin down (cyan) component at the Γ point from corresponding $N_{up}$ and $N_{down}$. One can see that profiles have their maximums at different binding energies which points to the opened Dirac point band gap. Spin measurements were acquired at room temperature (T = 300 K) which is significantly higher than temperature of magnetic ordering. Therefore, gap may exist even in paramagnetic phase. In [8] it explains by uncompensated spin fluctuation which can open a gap even above temperature of magnetic ordering. There is can be another technical explanation. From theoretical calculation [8] it was shown that the TSS is located close to the bulk conduction band and even have intersection with bulk valence band. For fig.1(a) it was also shown that lack of resolution makes the TSS undistinguishable from the bulk bands. In case of the spin out-of-plane component the same situation is also plausible.

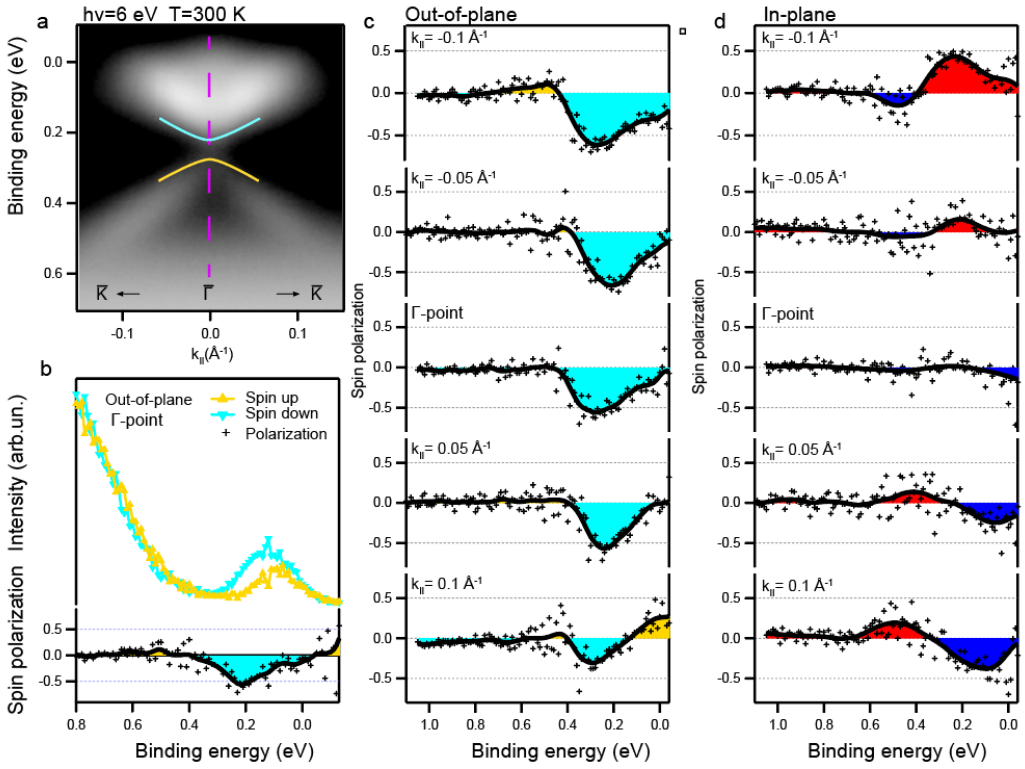


**Fig. 2 Spin-resolved ARPES data. a**, Spin-integrated ARPES spectrum taken at 6 eV photon energy along the K–Γ–K direction. Yellow and cyan curves show the location of the gapped TSS. **b**, Spin-resolved ARPES spectra taken at the Γ-point with respect to the out-of-plane spin quantization axis. The out-of-plane spin polarization is shown below the corresponding spin-up and spin-down spectra. **c**, **d**, Measured out-of-plane and in-plane spin polarization at different momentum values, respectively. The in-plane spin polarization changes its sign with $k_{II}$, as expected for the TSS. The measurements were performed at $T$ = 300 K.

Additionally, we study distribution of Mn states within the TSS energy region. With this intension we use resonant photoemission spectroscopy (ResPES) technic. Measurements at photon energy of an element adsorption level - on-resonance and at photon energy several eV higher/lower – off-resonance can highlight bands related to that element. For Mn we use 3d-3p resonance. In fig.3 (a) and (b) spectra at hv = 50 eV (on-resonance) and at hv = 48 eV (off-resonance) are presented. They we acquired at 1-squre endstation of Bessy II synchrotron (see Methods). Difference between on and off- resonance spectra and EDC at the Γ-point are presented in panels (c) and (d). One can see that the most absolute intensity increase is at about 4 eV binding energy which corresponds to Mn 3d band. Other part of EDCs are slightly modified and changes are visible only in case of relative difference plot (black curves in (d)). From the bottom part of (d) one can see that Intensity modifies only in the region between 1.2 to 0.5 eV binding energy, while the TSS is above 0.5 eV binding energy. Therefore, we can assume that there is no Mn density in the vicinity of the TSS opposite to the case of Mn doped $Bi_2Te_3$ [12].

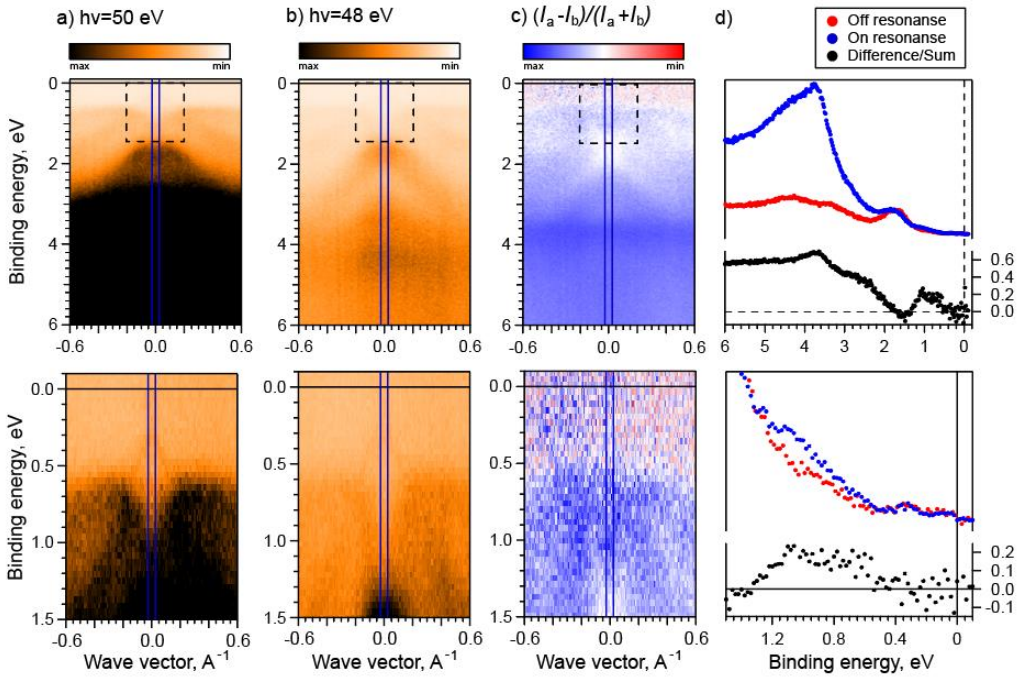


**Fig. 3** Resonant PES data. Columns (a) and (b) represent ARPES spectra measured on and off Mn 3d-3p resonance with photon energy of 50 eV and 48 eV respectively. Bottom parts show zoomed region near the TSS which marked by dashed lines in top parts. In column (c) the difference between on- and off- resonance spectra with normalization to their sum is presented. Positive value (blue) corresponds to the domination of on-resonance spectrum. EDCs at Γ-point for all spectra are shown in column (d).

## Conclusion

In the conclusion, we showed that electronic structure of MnBi2Te4 compound is characterized by the presence of a cone shape states in the vicinity of the Fermi level. We found that these states have the intensity dip between bottom and top parts. We relate this dip rather with bulk band gap or gap of mixed TSS and bulk density. Comparison of our ARPES spectra with theoretical calculations reveal unresolvable the TSS. By means circular dichroism and spin resolved measurements we showed spin inversion of the cone branches and prove their topological origin. Additionally, we found almost constant polarization along $k_{||}$ of out-of-plane spin component. Moreover, from the analysis of the spin resolved spectra at the Γ-point we showed a presence of the band gap at T = 300 K. Nevertheless, it also can be explained by the lack of energy resolution. By means of resonant PES we showed absence of the Mn density in the vicinity of the TSS.

## Methods

The experiments were carried out at 1-square and 1-cubed endstations of UE-112 Beamline and RGBL-2 station at BESSY II in Berlin. Samples recharacterization was made at Research Resource Center of Saint Petersburg State University “Physical methods of surface investigation”. Samples were cleaved in-situ at the base pressure of $6 \times 10^{-11}$ mbar. The crystalline order and cleanliness of the surface were verified by low energy electron diffraction (LEED) and X-ray photoelectron spectroscopy (XPS).

ARPES measurements were performed at 1-cubed and 1-square endstations of UE-112 beamline with sample temperatures down to 1 K (for 1-cubed) and about 25 K (for 1-square).

Spin-resolved ARPES measurements were performed at the RGBL-2 endstation using a hemispherical analyzer (Scienta R4000) and a photon energy of 6 eV. The photon beam was generated using the fourth harmonic of a custom-made femtosecondlaser system coupled to an ultrafast amplifier operating at a repetition rate of 100 kHz. The spin-resolved spectra were acquired with a three-dimensional Mott-type spin detector operated at 26 kV. The energy and angular resolutions of the spin-resolved measurements were 30 meV and 1.5° (corresponding to 0.02 $Å^{-1}$), respectively.

Resonant photoemission data were acquired at the 1-square endstations of UE-112 Beamline. The measurements were conducted at a base temperature of T = 25 K. The difference between on- and off-resonance spectra for the Mn 3p–3d transition corresponds directly to the density of the Mn 3d states. A photon energy series was conducted to determine suitable transition energies. The corresponding angle integrated spectra of on-resonance (hv = 50 eV) and off-resonance (hv = 48 eV) conditions can be seen in Fig. 3.

## References


[1] M. Z. Hasan and C. L. Kane, Rev. Mod. Phys. 82, 3045 (2010).
[2] F. D. M. Haldane, Phys. Rev. Lett. 61, 2015 (1988).
[3] C.-Z. Chang, J. Zhang, X. Feng, et al., Science 340, 167 (2013).
[4] Y. L. Chen, J.-H. Chu, J. G. Analytis et al., Science 329, 659 (2010).
[5] 4R. Yu, W. Zhang, H.-J. Zhang, S.-C. Zhang, X. Dai, and Z. Fang, Science 329, 61 (2010).
[6]X.-L. Qi, T. L. Hughes, and S.-C. Zhang, Phys. Rev. B 78, 195424 (2008).
[7] T. Hirahara, S. V. Eremeev, T. Shirasawa, et al., Nano Lett. 17, 3493 (2017).
[8] M. M. Otrokov, I. I. Klimovskikh, H. Bentmann et al., arXiv:1809.07389 (2018).
[9] M. Mogi, R. Yoshimi, A. Tsukazaki, et al., Appl. Phys. Lett. 107, 182401 (2019).
[10] E. V. Gomonay and V. M. Loktev, Low Temperature Physics 40, 17 (2019).
[11] R. S. K. Mong, A. M. Essin, and J. E. Moore, Phys. Rev. B 81, 245209 (2010).
[12] J. Sanchez-Barriga, A. Varykhalov, G. Springholz, et al., Nat. Comm., 7:10559, (2016).